

# Thermoelectric Properties of In<sub>0.3</sub>Ga<sub>0.7</sub>N Alloys

B.N. PANTHA,<sup>1</sup> R. DAHAL,<sup>1</sup> J. LI,<sup>1</sup> J.Y. LIN,<sup>2</sup> H.X. JIANG,<sup>2,4</sup> and G. POMRENKE<sup>3</sup>

1.—Department of Physics, Kansas State University, Manhattan, KS 66506-2601, USA.  
2.—Nano-Tech Center and ECE Department, Texas Tech University, Lubbock, TX 79409, USA.  
3.—Directorate of Physics and Electronics, Air Force Office of Scientific Research, Arlington, VA 22203-1768, USA. 4.—e-mail: hx.jiang@ttu.edu

We report on the experimental investigation of the potential of InGaN alloys as thermoelectric (TE) materials. We have grown undoped and Si-doped In<sub>0.3</sub>Ga<sub>0.7</sub>N alloys by metalorganic chemical vapor deposition and measured the Seebeck coefficient and electrical conductivity of the grown films with the aim of maximizing the power factor ( $P$ ). It was found that  $P$  decreases as electron concentration ( $n$ ) increases. The maximum value for  $P$  was found to be  $7.3 \times 10^{-4}$  W/m K<sup>2</sup> at 750 K in an undoped sample with corresponding values of Seebeck coefficient and electrical conductivity of 280  $\mu$ V/K and 93 ( $\Omega$  cm)<sup>-1</sup>, respectively. Further enhancement in  $P$  is expected by improving the InGaN material quality and conductivity control by reducing background electron concentration.

**Key words:** Thermoelectric (TE), InGaN, Seebeck coefficient, electrical conductivity, power factor

## INTRODUCTION

Thermoelectric (TE) devices convert heat energy directly into electrical energy without any moving parts. These devices produce no ozone-depleting gases and emit no radioactive radiation.<sup>1</sup> Recently, there has been much attention drawn to finding TE materials suitable for solid-state refrigeration and power conversion. The best TE materials for room-temperature application are Bi<sub>2</sub>Te<sub>3</sub>-based materials and structures,<sup>2,3</sup> but their applications are limited because tellurium is scarce, volatile, and toxic. Furthermore, the operational range of these materials is limited to temperatures less than  $\sim 100^\circ\text{C}$ . Therefore, the search of materials for TE applications beyond the tellurium-based compounds is necessary. Current research in thin-film TE materials without tellurium is concentrating on materials such as Si/Ge, SiGe/Si, and ErAs:InGaAs/InGaAlAs superlattices and SiGe alloys and trace of nitride alloys.<sup>4–11</sup> Thin-film TE materials are of great interest because they offer the potential for

direct integration of microcoolers/power generators with various photonic and electronic devices. The performance of TE devices is characterized by the material's TE figure of merit,  $Z$  ( $Z = P/\kappa$ , and  $P = S^2\sigma$ ), where  $P$ ,  $S$ ,  $\sigma$ , and  $\kappa$  are the power factor, Seebeck coefficient, electrical conductivity, and thermal conductivity, respectively. The power factor ( $P$ ) measures the electrical power generation capability, which is often used to assess the potential of the material for TE application. Since  $S$  and  $\sigma$  are interdependent, optimization of the product  $S^2\sigma$  is extremely important to obtain a high value of  $Z$ .

Although III-nitride materials have been extensively studied for visible and ultraviolet light emitters, detectors, and high-power transistors during the past decade, very little work has been done with respect to their thermoelectric properties.<sup>9–11</sup> Some of the outstanding features of III-nitrides that are highly attractive for TE applications include the ability for high-power and high-temperature operation, high mechanical strength, stability, and radiation hardness. Our recent study shows that high-In-content InGaN alloys could be potentially important TE materials.<sup>12</sup> The present work explores the potential of InGaN alloys as TE materials.

(Received July 28, 2008; accepted January 14, 2009;  
published online February 7, 2009)

The variations of power factor with electron concentration and temperature have been measured.

### EXPERIMENTAL PROCEDURES

Undoped and Si-doped In<sub>0.3</sub>Ga<sub>0.7</sub>N alloys, of thickness  $\sim 110$  nm, were grown on  $\sim 1\text{-}\mu\text{m}$  GaN/sapphire (0001) templates by metalorganic chemical vapor deposition (MOCVD). Ammonia (NH<sub>3</sub>), trimethylgallium (TMGa), trimethylindium (TMIn), and silane were used as precursors and dopants. The thickness of the films was estimated from *in situ* interference measurements during the epigrowth. The indium concentration was determined from the peak value of the x-ray diffraction (XRD) spectra of the (002) reflection in  $\theta$ - $2\theta$  scan mode and applying Vegard's law.

Seebeck coefficient and electrical conductivity measurements were performed by temperature gradient and van der Pauw Hall-effect measurement methods in the in-plane direction. Since InGaN was grown on a GaN/sapphire template, we performed two identical measurements in GaN/sapphire template (reference) and InGaN/GaN/sapphire sample (sample). The following two equations were used to extract the properties of the top InGaN film.<sup>13</sup>

$$\sigma_f = \frac{\sigma_s t_s - \sigma_r t_r}{t_s - t_r}, \quad (1)$$

$$S_f = \frac{S_s \sigma_s t_s - S_r \sigma_r t_r}{S_s t_s - S_r t_r}, \quad (2)$$

where  $\sigma$ ,  $S$ , and  $t$  stand for electrical conductivity, Seebeck coefficient, and layer thickness, respectively, and the suffixes f, s, and r stands for film, sample, and reference, respectively. A schematic illustration of the experimental setup for Seebeck coefficient measurement is shown in Fig. 1a. The

sample to be measured was cut into a rectangular shape ( $\sim 5$  mm  $\times$  20 mm). One end of the sample was placed on the sink while on the other end a heater was attached. On the surface of the sample, two thermocouples separated by  $\sim 8$  mm were attached. An in-plane temperature gradient was created along the sample by the heater. The Seebeck voltage and temperature gradients were measured by thermocouples. Temperature-dependent measurements were performed in a cryostat with a temperature range from 300 K to 750 K.

### RESULTS AND DISCUSSION

Figure 1b shows the measured Seebeck voltage ( $V_S$ ) of the samples with different electron concentrations ( $n$ ) at different temperature gradients. The slope of the linear fit of the data is the measure of the Seebeck coefficients ( $S$ ). Electrical conductivity ( $\sigma$ ) and  $S$  of the top InGaN layer were extracted using Eqs. 1 and 2, respectively. Figure 2a shows  $\sigma$  and  $S$  of In<sub>0.3</sub>Ga<sub>0.7</sub>N alloys as a function of  $n$ . The usual tradeoff behavior of  $\sigma$  and  $S$  is observed.  $S$  decreases while  $\sigma$  increases as  $n$  increases, as described by the following equations,<sup>14</sup>

$$\sigma = ne\mu, \quad (3)$$

$$S = \frac{k}{e} \left( r + \frac{5}{2} + \ln \frac{N_c}{n} \right), \quad (4)$$

where  $e$ ,  $\mu$ ,  $r$ ,  $N_c$ , and  $n$  are electronic charge, Hall mobility, scattering factor, effective density of states in conduction band, and electron concentration, respectively.

The variation of  $P$  with  $n$  is plotted in Fig. 2b. The plot shows that  $P$  increases as  $n$  decreases. The maximum value of  $P$  was found in an undoped sample ( $n \sim 7 \times 10^{18} \text{ cm}^{-3}$  measured at 300 K): which is  $\sim 2.8 \times 10^{-4} \text{ W/m K}^2$  at 300 K. The peak

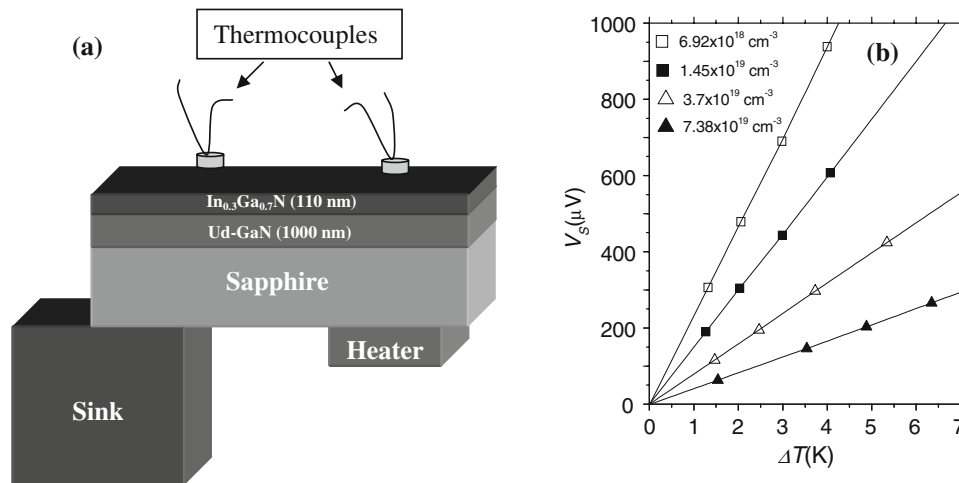


Fig. 1. (a) Schematic illustration of Seebeck coefficient ( $V_S$ ) measurement method. (b) Measured  $V_S$  of In<sub>0.3</sub>Ga<sub>0.7</sub>N/GaN/sapphire samples of different electron concentrations ( $n$ ) at different temperature gradients ( $\Delta T$ ).  $n$  in the plot is electron concentration of the top In<sub>0.3</sub>Ga<sub>0.7</sub>N layer measured by Hall-effect method.

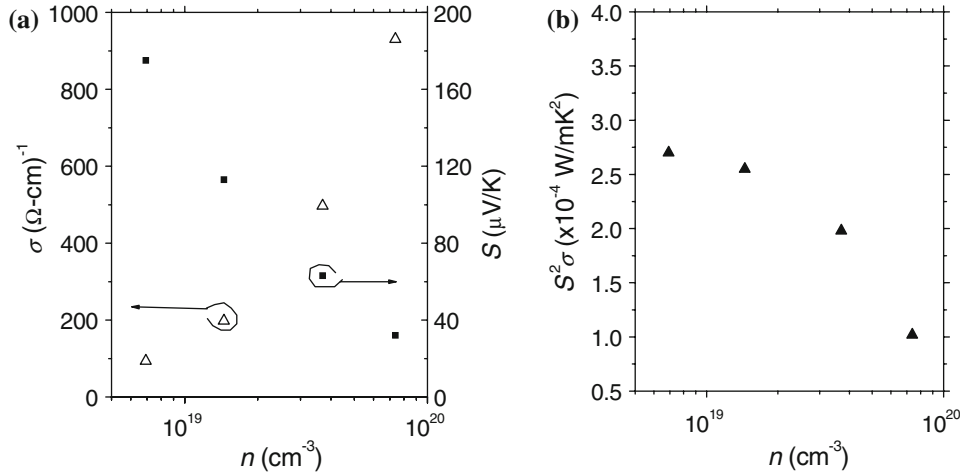


Fig. 2. (a) Electrical conductivity ( $\sigma$ ) and Seebeck coefficient ( $S$ ) as a function of electron concentration ( $n$ ) of  $\text{In}_{0.3}\text{Ga}_{0.7}\text{N}$  alloys and (b) power factor ( $S^2\sigma$ ) as a function of  $n$ .

value of  $P$  has yet to be found because further decreasing the carrier concentration is limited by the presence of a high background concentration of electrons, which arises from native defects such as oxygen and hydrogen impurities and nitrogen vacancies.<sup>15</sup> Recently, our group has demonstrated the mechanism for suppression of electron background concentrations and improving the quality of InN by using an AlN template and higher growth temperature.<sup>16</sup> The issue of high background concentration of electrons in InGaN alloys with relatively high In content is currently under intensive investigation,<sup>17,18</sup> and significant improvements in InGaN material quality and conductivity control are expected, which will lead to further enhancement in  $P$  in InGaN alloys with larger In content.

Temperature-dependent TE properties of  $\text{In}_{0.3}\text{Ga}_{0.7}\text{N}$  alloys were measured in the temperature range from 300 K to 750 K. Figure 3a shows  $S$  and  $\sigma$  of  $\text{In}_{0.3}\text{Ga}_{0.7}\text{N}$  alloy as a function of absolute

temperature ( $T$ ). It was found that  $S$  increases as  $T$  increases, whereas  $\sigma$  remains almost unchanged. The increase in  $S$  (regardless of no change in  $\sigma$ ) could be due to the electron hopping conductance at higher temperatures as described by Yamaguchi et al.<sup>10</sup> in InAlN and AlInGaN alloys. The maximum Seebeck coefficient was  $280 \mu\text{V/K}$  at 750 K. Temperature-dependent  $P$  is plotted in Fig. 3b, which shows that  $P$  increases as  $T$  increases. The maximum measured value of  $P$  was  $7.3 \times 10^{-4} \text{ W/m K}^2$  at 750 K. This value is about two times higher than that in  $\text{Al}_{0.35}\text{In}_{0.65}\text{N}$  and more than one order of magnitude higher as compared with that in  $\text{Al}_{0.26}\text{Ga}_{0.44}\text{In}_{0.30}\text{N}$ .<sup>10</sup> The results suggest that  $\text{In}_x\text{Ga}_{1-x}\text{N}$  alloys are better candidates for thermoelectric applications than other AlInGaN alloy systems. Our previous results also revealed that the dimensionless thermoelectric figure of merit ( $ZT$ ) of InGaN alloys are much higher than the reported values for other nitride materials.<sup>9,10,12</sup>

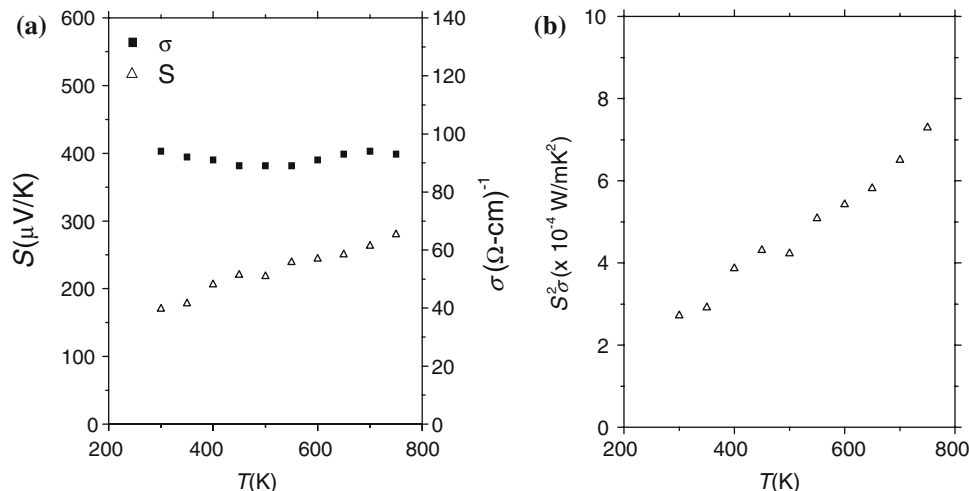


Fig. 3. (a) Electrical conductivity ( $\sigma$ ) and Seebeck coefficients ( $S$ ) as a function of temperature ( $T$ ) of  $\text{In}_{0.3}\text{Ga}_{0.7}\text{N}$  alloy with electron concentration  $\sim 7 \times 10^{18} \text{ cm}^{-3}$  and (b) power factor ( $S^2\sigma$ ) as a function of  $T$ .

## CONCLUSION

In summary, we have measured the thermoelectric properties of MOCVD-grown undoped and Si-doped In<sub>0.3</sub>Ga<sub>0.7</sub>N alloys. The power factor was observed to be maximum in an undoped sample. Further increases in power factor can be expected by reducing the background electron concentration and improving the material quality, which is the prime issue of recent investigation of InGaN alloys. It was found that the power factor increases as temperature increases with a maximum value of  $7.3 \times 10^{-4}$  W/m K<sup>2</sup> at 750 K.

## ACKNOWLEDGEMENTS

This work was funded in part by the US Air Force Office for Scientific Research (Grant No. FA9550-06-1-0441) and Department of Energy (Award No. 96ER45604).

## REFERENCES

1. G. Mahan, B. Sales, and J. Sharp, *Phys. Today* 50, 42 (1997).
2. M.G. Kanatzidis, S.D. Mahanti, and T.P. Hogan, *Chemistry Physics, and Materials of Science and Thermoelectric Materials* (New York: Kluwer Academic Plenum, 2002).
3. R. Venkatasubramanian, E. Slivola, T. Colpitts, and B. O'Quinn, *Nature* 413, 597 (2001).
4. B. Yang, W.L. Liu, J.L. Liu, K.L. Wang, and G. Chen, *Appl. Phys. Lett.* 81, 3588 (2002).
5. S.M. Lee, D.G. Cahill, and R. Venkatasubramanian, *Appl. Phys. Lett.* 70, 2957 (1997).
6. S.T. Huxtable, A.R. Abramson, C.L. Lin, A. Majumdar, C. laBounty, X. Fan, J.E. Bowers, A. Shakouri, and E.T. Croke, *Appl. Phys. Lett.* 80, 1737 (2001).
7. G. Zeng, J.E. Bowers, J.M.O. Zide, A. Majumdar, R. Singh, Z. Bian, Y. Zhang, and A. Shakouri, *Appl. Phys. Lett.* 88, 113502 (2006).
8. M. Takashiri, T. Borca-Tasciuc, A. Jacquot, K. Miyazaki, and G. Chen, *J. Appl. Phys.* 100, 054315 (2006).
9. S. Yamaguchi, R. Izaki, N. Kaiwa, and A. Yamamoto, *Appl. Phys. Lett.* 83, 5398 (2003).
10. S. Yamaguchi, R. Izaki, N. Kaiwa, and A. Yamamoto, *Appl. Phys. Lett.* 82, 2065 (2003).
11. W. Liu and A.A. Balandin, *J. Appl. Phys.* 97, 123705 (2005).
12. B.N. Pantha, R. Dahal, J. Li, J.Y. Lin, H.X. Jiang, and G. Pomrenke, *Appl. Phys. Lett.* 92, 042112 (2008).
13. W.L. Liu, T. Borca-Tasciuc, J.L. Liu, K. Taka, K.L. Wang, M.S. Dresselhaus, and G. Chen, *Proceeding 20th International Conference in Thermoelectric* (2001), p. 340.
14. K. Seeger, *Semiconductor Physics* (Berlin: Springer, 1999).
15. D.C. Look, H. Lu, W.J. Schaff, J. Jasiniski, and Z. Liliental-Weber, *Appl. Phys. Lett.* 80, 258 (2002).
16. N. Khan, A. Sedhain, J. Li, J.Y. Lin, and H.X. Jiang, *Appl. Phys. Lett.* 92, 172101 (2008).
17. C.G. Van de Walle and D. Segev, *J. Appl. Phys.* 101, 081704 (2007).
18. P.D.C. King, T.D. Veal, C.F. McConville, F. Fuchs, J. Furthmüller, F. Bechstedt, P. Schley, R. Goldhahn, J. Schörmann, D.J. As, K. Lischka, D. Muto, H. Naoi, Y. Nanishi, H. Lu, and W.J. Schaff, *Appl. Phys. Lett.* 91, 092101 (2007).